NUCLEAR STRUCTURE
(THEORETICAL)

NUCLEAR LEVEL DENSITIES

G. Bertsch and J. Wu

The effect of interactions on level densities is a poorly understood subject. The level density is usually parameterized in terms of the Fermi gas model, which involves as a parameter the single-particle density of states. The empirical values of this parameter,

$$g = \frac{\pi^2}{6} \frac{dn}{dE} \frac{A}{8\ \mathrm{MeV}}$$

differs from the infinite Fermi gas value by a factor of 2.[1]

It has been argued that the difference can be ascribed to static surface effects, based on the Thomas Fermi model.[2-5] It is easy to show, however, that static surface effects only increase the parameter by about 25%. The argument is based on the formula for the single-particle level density in a potential well derived by Siemens[6] and others. Describing the well by a function V(R,r), where R is a measure of the radius of the well (for example, the distance where the potential is half its maximum), the formula is

$$g(E_F) = \frac{4m}{2\pi^2\hbar^2}\left[\left(\frac{4\pi R^3}{3}\right)k_F + (4\pi R^2)\left(\delta(k_F) - \frac{\pi}{4}\right)\right] \quad (1)$$

where $\delta(k)$ is the phase shift of a wave with momentum k_F along the normal to the surface, and the phase shift is measured with respect to a sine wave that vanishes at r = R.

If the potential radius is defined so that $\delta(k_F) = \frac{\pi}{4}$, then there is no surface contribution to the level density and the naive Fermi gas formula can be applied. In Fig. 1 we show $\delta(k)$ for the usual Woods-Saxon potential,

$$V(R,r) = \frac{-50\ \mathrm{MeV}}{1+e^{(r-R)/0.65\ \mathrm{fm}}}$$

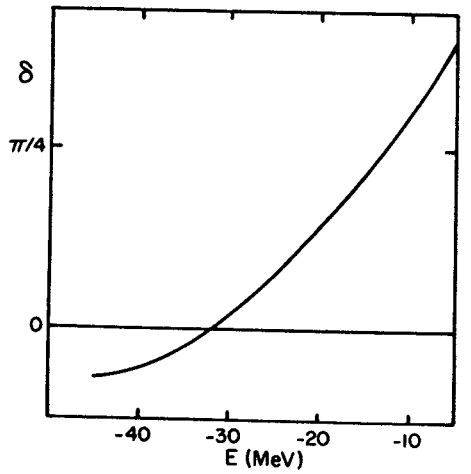

Fig. 1. Phase shift of bound state in semi-infinite Woods-Saxon potential, as a function of energy. The energy is measured with respect to zero binding for states with no momentum in the plane of the surface.

The phase shift goes through $\frac{\pi}{4}$ near the Fermi energy; thus the usual Woods-Saxon well radius gives the correct volume for the Fermi gas level density. Substituting $R = 1.25\ A^{1/3}$ fm, Eq. (1) yields

$$g(E_F) = \frac{A}{11.4}\ .$$

The momentum dependence of the Brueckner-Hartree nuclear potential reduces this by about 25%, so an effective mass enhancement of about a factor of 2 is needed to explain the empirical parameter. Since calculations of effective mass based on perturbation theory only give enhancements of 1.25-1.5, there remains a serious discrepancy.

We are presently investigating whether self-consistent Hartree-Fock theory provides a better treatment of level densities. We first calculate a ground state in Hartree-Fock theory together with the associated single-particle spectrum. The excited states are constructed by changing the occupation numbers of the single-particle states, and reminimizing the Hamiltonian. We expect that this will give a much compressed spectrum, compared to the independent particle model.

1. A. Bohr and B. Mottelson, Nuclear Structure, vol. 1, W.A. Benjamin, (1969) p. 188.
2. W. Stocker and J. Burzlaff, Nucl. Phys. A202, 265 (1973).
3. G. Sauer, H. Chandra and U. Mosel, Nucl. Phys. A264, 221 (1976).
4. M. Barranco and J. Treiner, Nucl. Phys. A351, 269 (1981).
5. M. Prakash, J. Wambach and Z. Ma, preprint (1982).
6. P. Siemens and A. Sobiczewski, Phys. Lett. 41B, 16 (1972).

SURFACE RESPONSE IN NUCLEI

H. Esbensen and G.F. Bertsch

The collective response of finite nuclei has been studied in great detail in the random phase approximation (RPA) using a shell-model representation. In order to obtain some of the global features of the surface response, avoiding the detailed dependence on shell structure, we study the response of a semi-infinite slab of nuclear matter. The free response of such a system has previously been used to study the importance of single-step processes in high energy inelastic proton scattering on heavy nuclei.[1]

The self-consistent RPA equation for the induced density $\delta\rho$ due to an external field V_{ext} is

$$\delta\rho(\bar{r},\omega) = -\int d\bar{r}' G_0(\bar{r},\bar{r}',\omega)\{V_{ext}(\bar{r}') + \delta V(\bar{r}',\omega)\}$$

where G_0 is the field-free Green's function and

$$\delta V(\bar{r},\omega) = \int d\bar{r}' v(\bar{r},\bar{r}')\delta\rho(\bar{r}',\omega)$$

is the induced potential originating from the residual interaction v. The formal solution is expressed in terms of the RPA Green's function:

$$\delta\rho(\bar{r},\omega) = -\int d\bar{r}' G_{RPA}(\bar{r},\bar{r}',\omega)V_{ext}(\bar{r}').$$

For an infinite system, as for example a free electron gas, this equation is easily solved in Fourier space. For finite nuclei it can be solved numerically on a finite grid in coordinate space.[2] For a semi-infinite system with a diffuse surface, which we consider, it can in general be difficult to obtain a solution. The problem is that a perturbation in the surface region will propagate into the interior of the slab, and a large residual interaction can lead to a strong coupling of bulk density oscillations and the surface response.

For a separable residual interaction, however, the RPA response of a semi-infinite slab can be reduced to closed integrals that can be evaluated numerically. In the figure we show the isoscalar and isovector response, together with the free response. Here we have chosen the separable residual interaction

$$v(\bar{r},\bar{r}') = \kappa \frac{\partial v}{\partial z}\circ\frac{\partial v}{\partial z}, \delta(\bar{r_n}-\bar{r_n'})$$

where V_0 is the single particle potential for the slab, and the strength κ has been chosen to simulate a realistic isoscalar/isovector residual interaction.

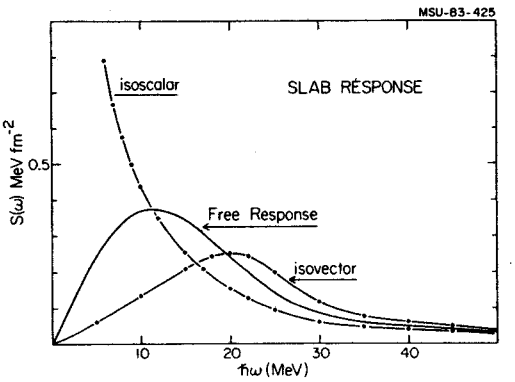

Fig. 1. The isoscalar response is seen to be enhanced for $\hbar\omega<10$ MeV, compared to the free response, and it diverges for $\hbar\omega\to 0$. For the isovector response, where the residual interaction is repulsive, the maximum of the response is shifted about 10 MeV to higher excitation energies. The sum of the energy-weighted response is the same for all three cases shown in the figure (energy-weighted sum rule). For the isoscalar response 25% of this sum is exhausted by excitations less than 10 MeV.

1. G.F. Bertsch and O. Scholten, Phys. Rev. C25, 804 (1982).
2. G.F. Bertsch and S.F. Tsai, Phys. Lett. 18C, 126 (1975).

THE GENERALIZED SENIORITY SCHEME

O. Scholten

A major problem in shell-model calculation for heavy nuclei is the size of the model space. Even a calculation for semiclosed shell nuclei involves dimensions of the order of several thousands. However, as has been pointed out by Talmi,[1] the generalized seniority (g.s) model provides a valid and powerful truncation scheme. Binding energy systematics and the excitation energy of the 2_1^+ level indicates that there is only a slight breaking of the g.s. scheme.

The g.s. scheme as it was proposed by Talmi is a generalization of the usual seniority concept[2,3] to the case of several nondegenerate orbits. In analogy to the treatment of the normal seniority formalism one introduces the operator

$$S_+ = \sum_j \alpha_j \frac{1}{2} \sqrt{2j+1}\, (a_j^\dagger a_j^\dagger)^{(0)} \qquad (1)$$

together with its adjoint $S_- = S^+$. Unlike the normal seniority scheme it is however not possible to complete this set of operators with an $S_0 = \frac{1}{2}[S_+, S_-]$ such that the three close under commutation. This means that there is no symmetry group associated with the g.s. scheme and thus that reduction formulas are much more complicated.[4] This has for a long time prohibited any extensive calculations. Also a problem arises in the definition of the basis states since, because of the lack of an underlying symmetry group, not a real g.s. quantum number can be introduced. A g.s. label, w, can be introduced by defining a w=0 state as

$$|\tilde{j}^{n=2N}\ w=0,\ J^\pi=0^+\rangle = S_+^N|0\rangle/K \qquad (2)$$

where K is an appropriately chosen normalization factor and S_+ is defined in Eq. 1. A w=2 state can now be defined as

$$|\tilde{j}^{n=2N}\ w=2, J^\pi\rangle = (S_+^{N-1}|j^2 J^\pi\rangle)_\perp/K' \qquad (3)$$

where the $\perp$ denotes that the stae is orthogonalized to the w=0 state in the case that J=0.

Excitation energies and transition rates can be calculated in the g.s. basis provided that the coefficients α_j are known that enter in the definition of the S_+ pair operator, Eq. 1. The α_j are determined by requiring that the Hamiltonian does not couple the w=0 stae with the w=2 states, i.e. that in a $w\leq 2$, J=0 basis the ground state is a pure w=0 state. To achieve this an iterative procedure has been developed that works as follows. For an arbitrary choice of the coefficients α_j the lowest energy state in a $w\leq 2$ basis can be written as $S_+'^{N-1}|0\rangle$ where the coefficients α_j' that enter on S_+ are different from the α_j that define S_+. The values α_j'' which replace α_j in the next iteration step are taken as a weighted average of α_j and α_j',

$$\alpha_j'' = ((N-1)\alpha_j + \alpha_j')/N \qquad (4)$$

Self consistency is reached when $\alpha_j = \alpha_j'$. In almost all cases we have considered, convergence was reached within five iteration steps even when the initial guesses for α_j were more than a factor two off from the final values. This diagonalization in the J=0 basis also yields energies and wave functions of excited J=0 states. Similarly a calculation in a w=0, J≠0 basis will give excited states with nonzero spin.

1. I. Talmi, Nucl. Phys. A172, 1 (1971).
2. G. Racah, Phys. 63, 367 (1943); 76, 1352 (1949).
3. A. de Shalit and I. Talmi, "Nuclear Shell Theory", Academic Press, N.Y. 1963.
4. O. Scholten and S. Pittel, Phys. Lett. 120B, 9 (1983).

THE TIN ISOTOPES IN THE GENERALIZED SENIORITY SCHEME

O. Scholten

As an application of the generalized seniority scheme[1] the Sn-isotopes have been calculated. As interaction a surface delta interaction (SDI) has been chosen in which the quadrupole component was enhanced by a factor F_2. The strength of the interaction A_1=0.18 and the quadrupole enhancement factor F_2=1.9 have been adjusted as to reproduce the 0-2-4 splittings in the ground state band. The enhancement of the quadrupole component finds its origin probably in core polarization which introduces components in the interaction between like particles that resemble the neutron-proton interaction, which has a strong quadrupole component.

Levels in the odd mass Sn isotopes can be calculated in lowest order in a generalized seniority w=1 basis. This calculation should reproduce the lowest levels with spin and parity equal to the single particle (s.p.) states included in the calculation insofar as they are strongly populated in s.p. transfer. In the calculation of the w=1 states in the nucleus (A+1) the structure of the S-pair state (Ref. 1) is taken the same as what has been determined for the nucleus (A+2). The single particle energies, listed in Table I, have been adjusted as to give a best agreement for the low-lying levels in the odd-mass Sn isotopes, and the results of the calculation are compared with experiment in Fig. 1. Since binding energies are not considered, the s.p. energy for the $g_{7/2}$ orbit is arbitrarily normalized to 0.0. The calculated energies of the 2_1^+ and 4_1^+ levels are compared with experiment in Fig. 2.

A calculation of binding energy systematics, electromagnetic transition rates and single particle transfer amplitudes is in progress.

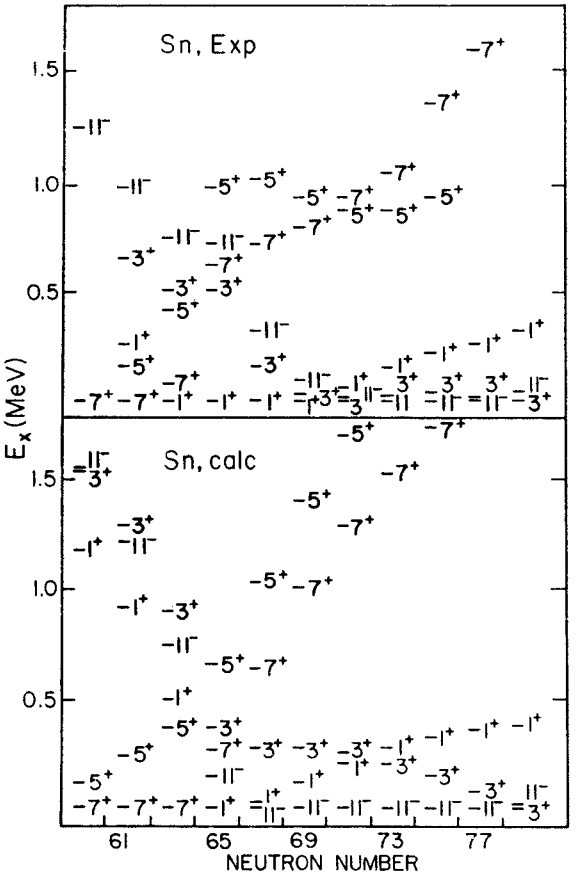

Fig. 1. Some calculated and experimental energies for the odd-mass Sn isotopes. The levels are labelled with twice the level spin .

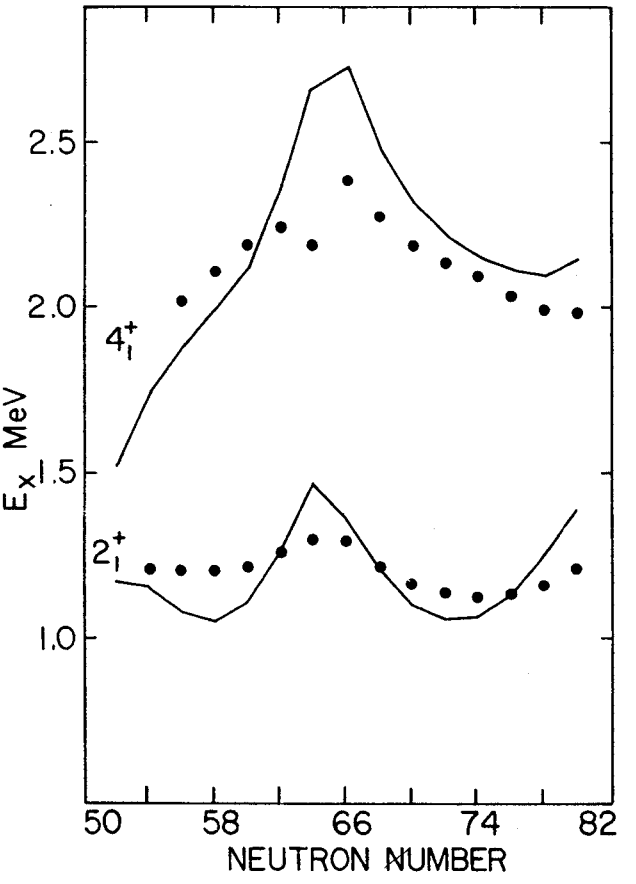

Fig. 2. The calculated and experimental energies for the 2_1^+ and 4_1^+ levels in the even-mass Sn isotopes.

Table I. Determined single particle energies for the Sn isotopes

j	$g_{7/2}$	$d_{5/2}$	$d_{3/2}$	$s_{1/2}$	$h_{11/2}$
ε_j	0	-0.5	2.0	1.5	2.4

1. O. Scholten, contribution to this annual report.

THE N=82 ISOTONES IN THE GENERALIZED SENIORITY SCHEME

O. Scholten and H. Kruse

An extensive calculation of the N=82 isotones has been done in the shell model.[1] This calculation has resulted in a set of single particle energies and two-body matrix elements which optimally reproduce the observed binding and excitation energies. For members of the N=82 isotone chain above A=140 the calculations become very time-consuming. In a basis which has been truncated on seniority ($v \leq 4$), and in which the occupation of the $h_{11/2}$ orbit is restricted, one routinely has to handle matrix dimensions of 1000-2000; the largest dimensions are of the order of 3500.

In order to recover some of the simplicity, the calculations have been repeated in the generalized seniority scheme,[2] and the results of this comparison for excitation energies are reported elsewhere.[3] The agreement between the two calculations for low-lying levels is impressive, especially in view of the fact that the generalized seniority scheme involves matrix dimensions of not more than 10.

We report here on calculation of electromagnetic transition rates in the N=82 isotones. In Fig. 1 the $B(E2;2^+ \rightarrow 0^+)$ calculated in both the shell model and the generalized seniority scheme are compared to experiment. The shell model values were obtained using Wood-Saxon wave functions and an effective charge $e_{eff}=1.67$; the calculation in the generalized seniority scheme uses oscillator wave functions and an effective charge $e_{eff}=1.52$. Both calculations give similar results for the lower-mass members of the isotone chain, the shell model results reproduce the data slightly better for A=144.

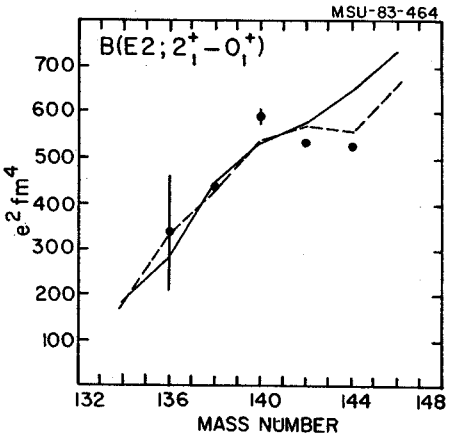

Fig. 1. Experimental and computed B(E2) values for the $2^+)1$ to $0^+)1$ transition in the N=82 isotones. The solid line represents the calculation in the generalized seniority scheme, the dashed line shows the shell model results.

The observed trends in the B(E2) can be easily understood in the generalized seniority scheme: For the lighter isotopes the B(E2) value increases linearly with mass since the $B(E2;2^+ \rightarrow 0^+)$, which connects states that differ in seniority, is proportional to the number of fermion pairs in the valence shell. If Z=64 were a good shell closure, the B(E2) would decrease linearly for $57<Z<64$, since increasing the number of protons decreases the number of holes in the 50-64 subshell. Assuming no subshell closure at Z=64, the B(E2) would increase linearly from Z=50 to Z=66. As can be seen from Fig. 1, the B(E2) values displays a trend somewhat in between these two extremes; this can be understood in terms of an effective number of fermion pairs as described in Ref. 4.

1. H. Kruse and B.H. Wildenthal, Bull. APS, 27, 533 (1982); BAPS 27 725 (1982)
2. O. Scholten, contribution to this report.
3. O. Scholten and H. Kruse, Phys. Lett. 125B, 113 (1983).
4. O. Scholten 127B (ig83)144.

THE ODD-MASS PLATINUM ISOTOPES IN THE IBFA MODEL

O. Scholten and Y. Lee

The Platinum isotopes have always formed interesting test cases for the IBA model and formed the first evidence for the occurrence of the O(6) symmetry in nuclei. Recently the interest in the Pt isotopes has been revived with the introduction of super-symmetries. Several different reduction schemes for these super-symmetries have been proposed. Super-symmetries offer a simple framework for labeling the states in a nucleus and dictate selection rules for transition. From a microscopic point of view symmetries are often very ad hoc and difficult to understand. For this reason we are calculating the spectra of the odd Pt-isotopes in the IBFA model. In this contribution only preliminary results of the calculation for ^{195}Pt will be reported.

In the IBFA model ^{195}Pt is calculated by coupling the degrees of freedom of a single neutron hole to the systems of bosons describing the even-even core, ^{196}Pt. In the discussion of negative parity levels only the single particle levels close to the Fermi surface, i.e. the $p_{1/2}$, $p_{3/2}$ and $f_{5/2}$ orbits will be important. In the IBFA calculation the occupancies of these levels was taken as v^2=.7, .8, .72 with relative single particle energies ε_j=0.0, .35, .22 for the $p_{1/2}$, $p_{3/2}$ and $f_{5/2}$ orbits respectively. The strength of the boson-boson quadrupole and exchange force were taken as BFQ=0.3, BFE=0.9. The value of the χ parameter appearing in the quadrupole interaction has been taken the same as the value of χ_ρ in the fit to the even Pt isotopes, CHQ = -0.8. In Fig. 1 the calculated energies are compared with experiment and those of a recent super-symmetry calculation.[1] Both calculations agree with the data almost equally well. Also the pattern of the B(E2) from the ground state $1/2^-$ to the first 5 excited states is reproduced in both calculations. In spite of all this agreement the overlap of the wave function for the ground state $1/2^-$ state obtained from the two calculations is only about 0.5, showing that the two calculations differ considerably. In order to distinguish between the two models a systematic calculation of all known odd Pt-isotopes is in progress comparing not only energies but also electromagnetic transitions and single particle transfer amplitudes.

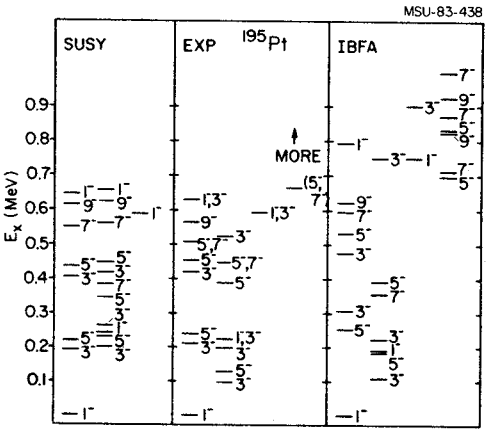

Fig. 1. The experimental spectrum[2] for ^{195}Pt is compared with the super-symmetry calculation[1] and and IBFA calculation. The levels are labelled with twice the spin.

1. H.Z. Sun, A. Frank and P. van Isacker, Phys. Rev. C27, 2430 (1983).
2. D.D. Warner, R.F. Casten, M.L. Stelts, H.G. Borner and G. Barreau, Phys. Rev. C26, 1921 (1982).

IBFA CALCULATION FOR THE PROMETHIUM ISOTOPES

O. Scholten and T. Ozzello

The Interacting Boson-Fermion Model (IBFM) is used to describe the spectra and electromagnetic properties of odd-even nuclei. In the model the spectrum of an odd-even nucleus is described by coupling the degrees of freedom of an odd particle to an even-even nucleus which is calculated in the Interacting Boson Model (IBM). We have applied the IBFM to the odd-mass promethium isotopes. Extensive calculations for the neighboring europium isotopes in the framework of IBFM have been published.[1] Comparison of the parameters can yield the proton dependence of the IBFM parameters.

Two separate sets of calculations are done, one for the positive and one for the negative parity levels. To calculate the negative parity levels an $h_{11/2}$ proton is coupled to the neodynium core for which there exists an IBM calculation[2]. Figure 1 shows the comparison between the calculation and experiment. Three parameters, of which only two are linearly independent, are used to calculate these levels, VSQ, which gives the

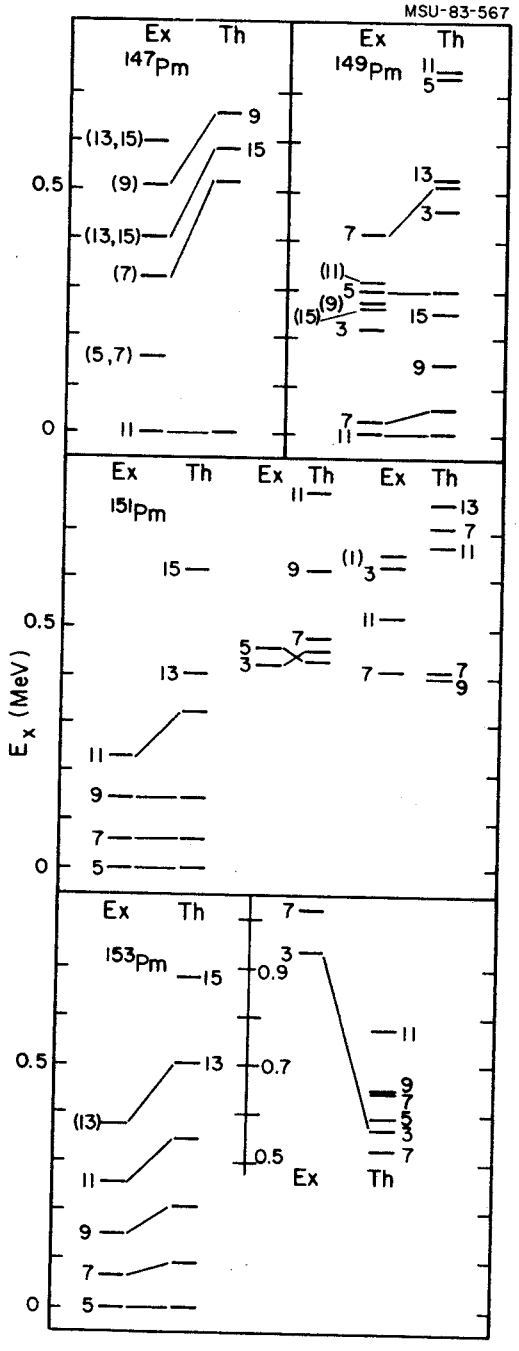

Fig. 1. Experimental and calculated negative parity levels of the odd-mass Pm isotopes. The levels are labelled with twice the spin.

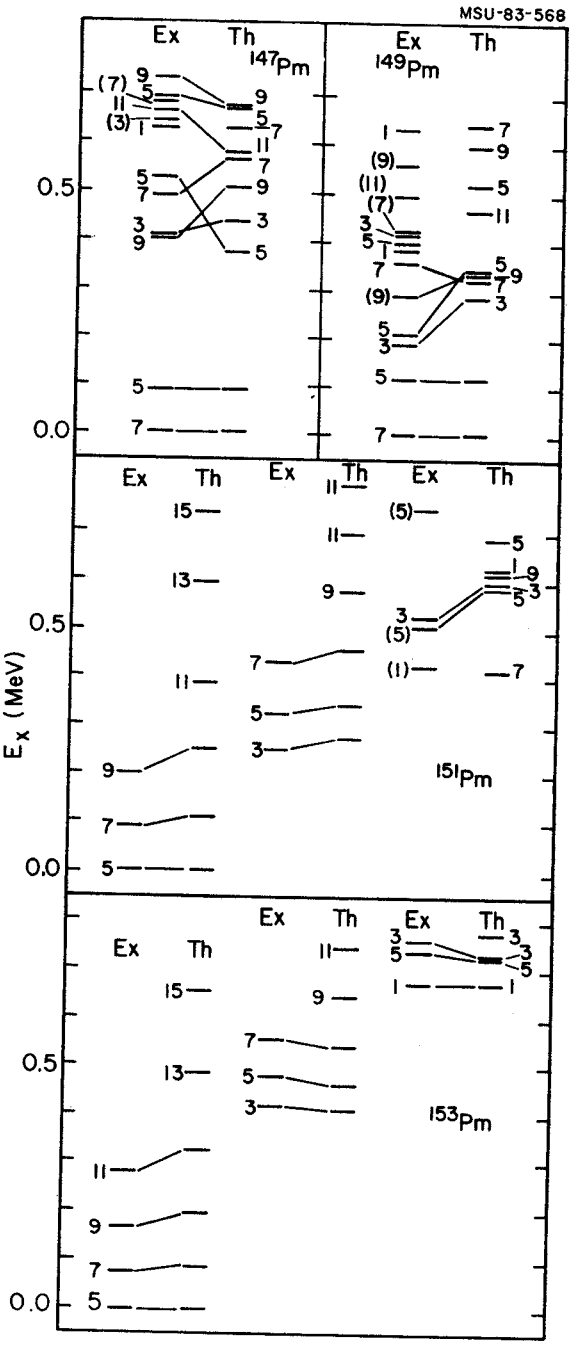

Fig. 2. Experimental and calculated positive parity levels of the odd-mass Pm isotopes.

occupational probabilities of the $11/2^-$ proton orbit, (A_0), the strength of the exchange force, and (Γ_0), the strength of the quadrupole-quadrupole interaction. These parameters all vary smoothly as a function of neutron number as predicted by the microscopic calculation. The positive parity levels were calculated by coupling a $d_{5/2}$ and a $g_{7/2}$ proton to the neodynium core. The levels agree with the experimental values as shown in Fig. 2. The same parameters are used for this calculation, with the addition of a new parameter, PEN, which gives the relative quasi-particle energies for the $5/2^+$ and $7/2^+$ proton orbits. The occupancies for the two orbits are taken differently. These parameters all vary smoothly with neutron number. Calculations were also done to obtain values for single particle transfer amplitudes, B(E2) and B(M1) transitions, along with magnetic and quadrupole moments.

1. O. Scholten and N. Blasi, Nucl. Phys. A380, 509 (1982).
2. O. Scholten, Ph.D. Thesis, University of Groningen, The Netherlands (1980).

THE ODD-MASS IRIDIUM ISOTOPES IN THE IBFA MODEL

O. Scholten and T. Ozzello

In the IBFA model the odd-mass Ir isotopes (Z=77) are calculated by coupling the degrees of freedom of the odd proton to the Pt(Z=78) core with the same number of neutrons. In the description of the positive parity levels the $s_{1/2}$ and $d_{3/2}$ orbits will play a dominant role. The positive parity levels have been calculated before in a super symmetry model[1] where only the coupling of a $d_{3/2}$ proton hole to an O(6) core is considered. This model can explain binding energies and B(E2) selection rules quite well. Single particle transfer amplitudes[2] however indicate that already the $1/2_1^+$ level at $E_x \approx 50$ keV contains a considerable $s_{1/2}$ component. For this reason we have started IBFA calculations in which both the $s_{1/2}$ and the $d_{3/2}$ orbits are being considered.

In the calculation the parameters in the IBFA Hamiltonian have been adjusted from isotope to isotope so as to give a best agreement for excitation energies. The parameters are listed in Table I. The calculated excitation energies are compared with experiment in Fig. 1. In this calculation the $1/2_1^+$ level contains a considerable $s_{1/2}$ component. A detailed calculation of spectroscopic factors and electromagnetic transition rates is in progress.

MSU-83-476

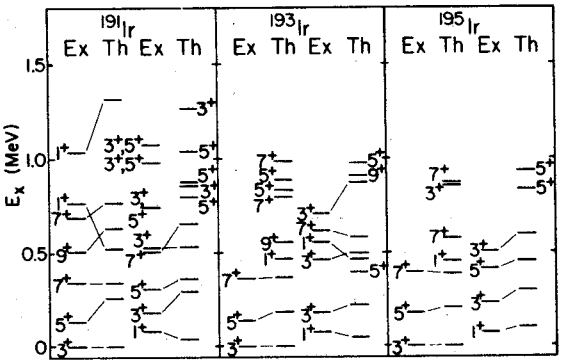

Fig. 1. Calculated and experimental excitation energies for ^{191,193,195}Ir.

1. F. Iachello and S. Kuyucak, Ann. Phys. 136, 19 (1981).
2. J.A. Cizewski, D.G. Burke, E.R. Flynn, R.E. Brown and J.W. Sunier, Phys. Rev. C27, 1040 (1983).

Table 1. Parameters used in the Ir Calculation.

A	191	193	195
Γ_0	.30	.30	.60
Λ_0	.70	.60	.80
$v^2 s_{1/2}$	.25	.25	.25
$v^2 d_{3/2}$	.25	.25	.25
$\varepsilon_{s_{1/2}} - \varepsilon_{d_{3/2}}$	.1	.1	.25

B(E2) VALUES AND LEVEL ENERGIES OF EVEN-MASS STABLE DY NUCLEI IN THE IBA MODEL

R. M. Ronningen, O. Scholten, and T. Ozzello

It was noted in early Coulomb excitation and inelastic deuteron scattering studies of deformed rare-earth region nuclei that E2 and E3 excitations of vibrational-like $I^{\pi}=2^{+}$ and 3^{-} states were, in general, stronger for increasingly more neutron deficient isotopes of a given nucleus. More recent Coulomb excitation studies confirmed this(for discussion and references see Ref. 1). In particular, in the lightest isotope of each stable even-A Gd, Dy, Er, Yb, and Hf nucleus the I^{π} $K=2^{+}2$ state has the largest B(E2) value to the ground state. The strength and level energy of this "gamma" vibrational state remains fairly constant throughout the region, except for the Yb nuclei. On the other hand, the lowest lying I^{π} $K=2^{+}0$ states(traditionally called beta vibrational states), show some collectivity (~1 single particle unit) only in the lightest isotopes. In fact, in the above nuclei the lightest isotope has the most collective $I^{\pi}K=2^{+}0$ state, except in the case of the Dy nuclei. The level energies generally increase rapidly with increasing neutron number and this particular mode of excitation seems to disappear in the heaviest isotopes.

The stable Dy nuclei should provide interesting tests of nuclear models because their intrinsic shapes range from weakly (N=90) to strongly deformed (N=98), the general behavior of the low-lying vibrational-like states described above, and particularly because of the apparently anomalously small collectivity exhibited by the I^{π} $K=2^{+}0$ vibrational state in ^{156}Dy compared to the other lightest nuclei, specifically the isotones ^{154}Gd and ^{162}Er. We have thus chosen to investigate the Dy nuclei using the IBA model.

The level energies and B(E2) values of the even mass Dy isotopes have been calculated in the IBA-1 model using the Hamiltonian where

$$H = \varepsilon n_d + \frac{1}{2}\kappa\,(L^{(1)}\cdot L^{(1)}) + \frac{1}{2}\kappa'\,(Q^{(2)}\cdot Q^{(2)}),$$

$$L^{(1)} = \sqrt{10}\;(d^{+}\tilde{d})^{(1)},$$

and

$$Q^{(2)} = (s^{+}\tilde{d} + d^{+}\tilde{s})^{(2)} + \frac{\chi}{\sqrt{5}}\;(d^{+}\tilde{d})^{(2)}$$

The four parameters $\varepsilon,\kappa,\kappa'$, and χ (listed in Table I) were adjusted for each isotope separately, however insisting on a smooth dependence of the parameters on mass number. The decrease in χ indicates the transition from an axially symmetric rotor to a γ-unstable shape. In the level energy spectrum shown in Fig. 1 this can be seen from the low-lying $2^{+}2$ level in comparison to the "β-band". The trends of the level energies are well reproduced.

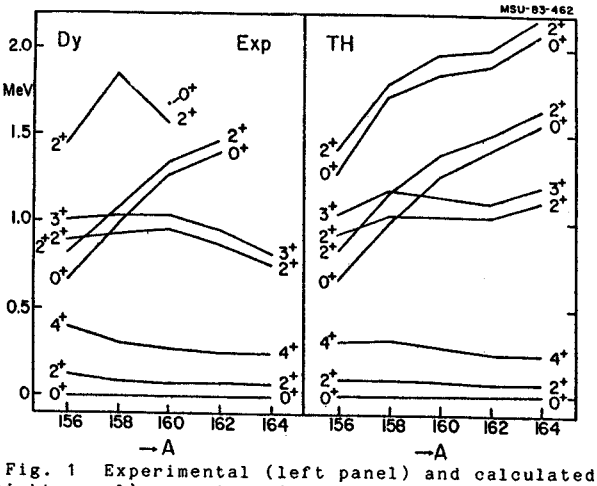

Fig. 1 Experimental (left panel) and calculated (right panel) energies of low-lying levels in the stable even mass Dy isotopes.

In the IBA model the number of bosons is usually chosen as the number of fermion pairs outside of a closed shell. In the case of Dy (Z=66) the choice of closure is ambiguous. A calculation[2] of the effective number of bosons suggests that the number of proton bosons should be taken as 4, instead of 8 if Z=50 or 1 if Z=64 is taken as the closed shell.

The B(E2) values were calculated using the quadrupole operator $Q^{(2)}$ as the transition operator. We used the value $\chi=-1.5$ for all isotopes. As can be seen in Fig. 2 the trends of B(E2) ratios are well reproduced but the increase of $B(E2;2_1^{+} \rightarrow 0_1^{+})$ is overpredicted. The reason for this could be that also for neutrons the concept of an effective boson number should be introduced. Apparently these numbers should be smaller than the ones used in the present calculations.

1. R.M. Ronningen, R.S. Grantham, J.H. Hamilton, R.B. Piercey, A.V. Ramayya, B. van Nooijen, H. Kawakami, W. Lourens, R.S. Lee, W.K. Dagenhart, and L.L. Riedinger, Phys. Rev C 26, 97(1982).
2. O. Scholten, Phys. Lett. 127 B, 144 (1983)

Table I. Parameters used in the IBA calculations of the Dy isotopes

A	156	158	160	162	164
E	0.295	0.266	0.133	0.0	0.0
κ	0.0025	0.0025	0.0025	0.0025	0.0025
κ'	-0.0413	-0.0518	-0.0585	-0.0585	0.0585
χ	-2.50	-2.00	-1.50	-1.33	-1.33

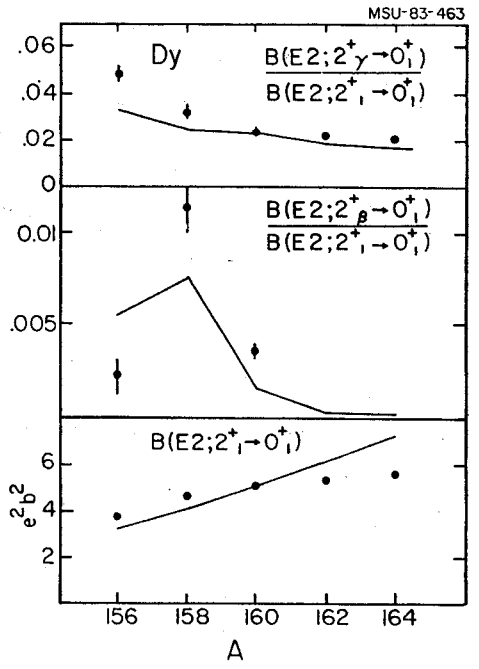

Fig. 2 Experimental and calculated B(E2) values for the stable even mass Dy isotopes.

ELASTIC MAGNETIC ELECTRON SCATTERING FROM p SHELL AND sd SHELL NUCLEI

R. Radhi, B. A. Brown and B. H. Wildenthal

We have calculated the form factors for elastic magnetic electron scattering from all stable nuclei below A = 40 which have non zeroground state spins. These form factors provide very detailed and specific information about the structure of the nuclear states which are probed. Comparisons of model predictions with experimental data thus yield important critiques of the theoretical descriptions of these states. We have used such comparisons to test the shell model wave functions recently derived for the p- shell and sd-shell regions (Ref 1, Ref 2). These wave functions result from calculations which assume that the two-body matrix elements of the effective model Hamiltonian decrease with increasing A as a power of (1/A).

We have pursued these comparisons of theoretical with experimental form factors beyond the arena of tests of specific shell model configuration mixing in order also to investigate the role of higher-order corrections to the basic elements of the shell-model ansatz. Specifically, we have tested the degree to which changes in the values of the magnetic g-factors in the conventional expressions of the magnetic operators affect the predicted form factors. We have also studied the dependence of the calculated form factors upon the radial dimensions of the single-particle wave functions which form the basis of the shell model.

The "single-particle" nuclei, those which correspond to one nucleon more or less than a "magic" closed shell nucleus such as ^{16}O or ^{40}Ca have particularly simple features in the conventional shell-model representation. The wave functions for their ground states are just single-particle orbits and are hence independent of the interference effects of the configuration mixing induced by the residual two-body Hamiltonian. Within the confines of the usual shell-model assumptions, then, deviations between theory and experiment for the single-particle nuclei are immediately attributable to the sort of higher-order effects mentioned above.

Elastic magnetic form factors calculated for ^{17}O are shown (solid lines) in Fig. 1 in comparison with experimental data (Ref 3). The model wave function employed in the calculation is that of a $0d_{5/2}$ neutron. We use a representation (Ref 4) which allows us to display the conventional magnetic moment along with the electron scattering data. The left-hand panels of Fig. 1 show predictions based on harmonic oscillator radial dependence while the right-hand panels show the corresponding results based on a

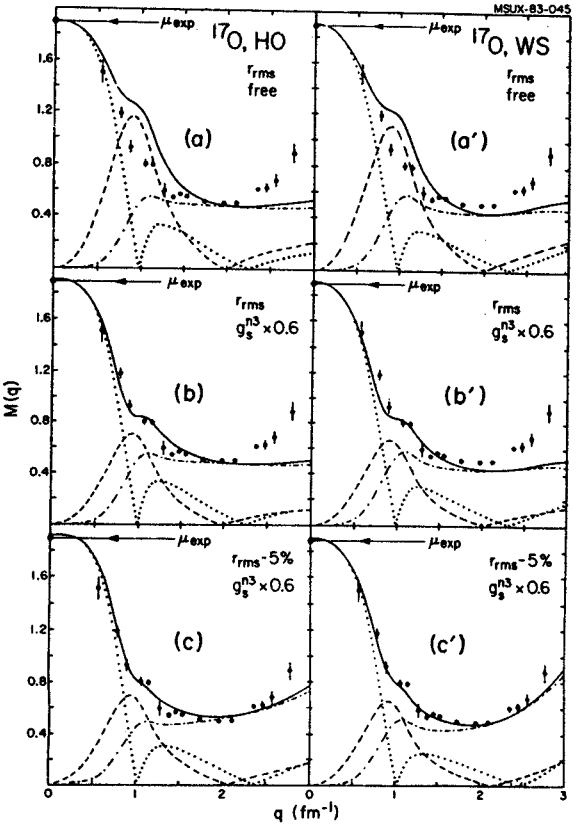

Fig. 1. Comparison of experimental and theoretical elastic magnetic scattering form factors and magnetic moments for ^{17}O. See text for details.

Woods-Saxon potential radial dependence. In both instances the scales of the radial wave functions are set originally to reproduce the measured charge radius of ^{17}O. It can be seen that in all instances there is little substantive difference between the harmonic oscillator and Woods-Saxon results.

The top panels show the results which are obtained by giving the g-factors which enter into the conventional formulations of the operators for the various magnetic multipoles the value measured for the free neutron. The theoretical results reproduce the measured magnetic dipole moment of ^{17}O, a fact long well known. They deviate from the experimental scattering data in the regions of momentum transfer q around 1.0 fm^{-1} (theory larger than experiment) and 2.5 fm^{-1} and greater (theory smaller than experiment). The contributions of the various magnetic multipoles to the theoretical form factors are indicated in Fig. 1 by the dotted lines (M1), the dashed lines (M3) and the the dashed-dotted lines (M5). The sums of the squares of these contributions give the squares of the total form factor values. The lines show the absolute values of these individual multipole amplitudes. We see from these decompositions that the M3 contribution dominates in the 1.0 fm^{-1}

region and that the M5 contribution dominates at beyond 2.0 fm^{-1}.

The middle panels of Fig. 1 shows the results of using a value of g_s in the M3 operator which is 0.60 times the free neutron value. This has the simple consequence of reducing the (M3 dominated) form factor in the region of 1.0 fm^{-1} to approximately the measured magnitudes. This change leaves both the lower q and higher q portions of the calculated form factors essentially unchanged. No such simple scaling of g-factors can rectify the disagreement between theory and experiment at the highest q values, however. One simple alteration to the conventional values of the basic shell-model parameters can remove most of the high q discrepancy. This alteration is to use a $0d_{5/2}$ single-particle wave function whose rms radial size is 0.95 times the "conventional" value. The "conventional" value is determined by reproducing the measured rms charge radius under the assumption that all occupied single-particle states of the shell model (including both "core" and "active" orbits) are generated from a single parametrization of the single-particle potential.

The bottom panels of Fig. 1 show the effects of using this reduced radius for the $0d_{5/2}$ wave function in conjunction with the quenched value of g_s for the M3 multipole. Both the harmonic-oscillator and Woods-Saxon versions of this prescription of the model form factor agree well, by our standards, with the measured moment and form factor data. We are left with questions about the significance of these alterations of "conventional" parameters which have the effect of improving agreement between the predictions of the single-particle model and experiment. Are the adjustments needed for ^{17}O merely ad hoc compensations for an overly simple model and in themselves devoid of physical significance? Or, do they provide a concise summary of the observable consequences of the single-major-shell model approximation which can be related to theoretical estimates of the higher-order corrections to this conventional picture of nuclear structure?

The obvious next step in this inquiry is to examine the case of ^{39}K, the nucleus which corresponds to a single vacancy ($d_{3/2}$) in the sd-shell. In Figs. 2 and 3 we pursue the same issues of g-factor renormalization and single-particle wave function radius. In Fig. 2a we show the predictions of the "standard model", in which the $0d_{3/2}$ proton is assumed to have its free-space g-factor and an harmonic-oscillator radial wave function with a radius which is consistent with the measured charge radius of the nucleus. The experimental data is from Ref 5 [circles-(Amsterdam data) and squares-(Bates data)]. The case of ^{39}K has an extra degree of complexity relative to ^{17}O in that the charge of the proton contributes a current term which is absent to lowest order in the case of the single neutron of ^{17}O. The bottom two panels of Fig. 2 show the individual spin and orbital contributions to the total form factor presented in the top left panel. We plot absolute values, and the spin contribution shown in the bottom right panel is negative at q-values of less than 0.7 fm^{-1}. The well-known result that the small magnetic moment of ^{39}K results from a cancellation of the spin and orbital contributions is evident from Fig. 2 as is the fact that the spin contribution dominates the scattering at large momentum transfers.

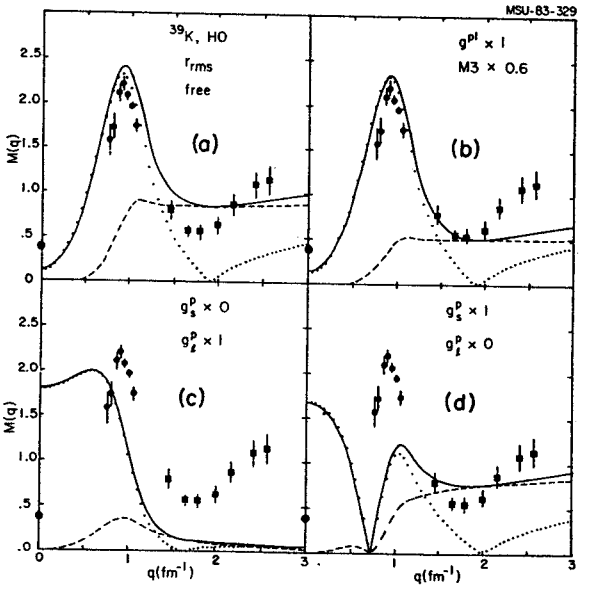

Fig. 2. Comparison of experimental and theoretical elastic magnetic scattering form factors and magnetic moments for ^{39}K. See text for details.

Inspection of Fig. 2a shows that the standard prediction misses the value of the moment, is too large at the peak around 1.0 fm^{-1} and at the valley around 1.5-2.0 fm^{-1}, and does not reproduce the slope of the data at still larger q values. The top right panel shows that multiplying the M3 g-factors by 0.6, the same factor used for ^{17}O, improves the agreement between calculated and measured form factors in the vicinity of q ≈ 1.5 fm^{-1}. This alteration has no appreciable effect on the other aspects of the correspondence. In particular, the deviation of the calculated slope from that of the data at large momentum transfers is made more strikingly evident. We have quenched both the orbital and spin M3 g-factors in the result shown in Fig. 2b. The relatively small contribution from the orbital term renders this choice essentially equivalent to the alternative of quenching only the spin contribution.

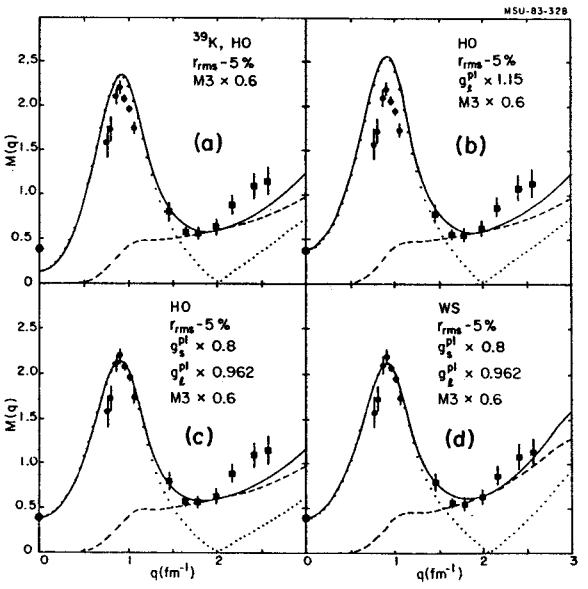

Fig. 3. Comparison of experimental and theoretical elastic magnetic scattering form factors and magnetic moments for ^{39}K. See text for details.

In Fig. 3 we illustrate the effects of altering the radius of the single particle wave function and of making more detailed alterations in the M1 g-factor renormalizations. As should be expected, the use of a smaller radius parameter causes the calculated values to increase at large momentum transfers and, hence, to agree better with the data. Either the spin or the orbital term can be altered to bring the calculated and measured dipole moments into agreement with each other. Not all such choices are consistent with the scattering data, as is shown by Fig. 3b, where the results of increasing the orbital g-factor by a factor of 1.15 and leaving the spin g-factor unchanged are compared with experiment. Fig. 3c shows the results of a combination of renormalized M1 spin and orbital g-factors which agrees reasonably well with both moment and scattering data. Fig. 3d shows the same calculation as in Fig. 3c, but in this case Woods-Saxon rather than harmonic oscillator radial wave functions have been used. The best agreement with experiment is obtained by this last calculation.

Similar calculations for all magnetic elastic form factors for the p and sd shell nuclei have been carried out and compared to experiment where available (Ref 4). Away from the closed shells the additional effects of configuration mixing are essential in interpreting the comparison between experiment and theory (Ref 6).

1. C. Chitwood, H. Kruse and B. H. Wildenthal, unpublished.
2. B. H. Wildenthal, Bull. Am. Phys. Soc. 27, 725 (1982).
3. M. V. Hynes et al., Phys. Rev. Lett. 42, 1444 (1979).
4. R. Radhi, Phd. Thesis, Michigan State University, 1983.
5. L. Lapikas, Proc. of the International Conference "Modern Trends in Elastic Electron Scattering", published by IKO Amsterdam 1978, p. 49.
6. B. A. Brown, R. Radhi and B. H. Wildenthal, to be published in Phys. Lett. B.

INELASTIC ELECTRON SCATTERING FROM ^{27}Al

R. Radhi, B.A. Brown and B.H.Wildenthal

Recent measurements by Ryan and co-workers[2] of the inelastic scattering cross sections of electrons from ^{27}Al sample extensive ranges of excitation energy and momentum transfer q and are characterized by exceptionally good energy resolution and freedom from background contamination. They hence provide a rich field within which to test theories of nuclear structure with precision and thoroughness. We compare the results of this experiment with predictions of longitudinal and transverse electron scattering form factors derived from wave functions obtained in a new shell-model calculation for the positive-parity states of ^{27}Al. This new calculation employs the full $0d_{5/2}$-$1s_{1/2}$-$0d_{3/2}$ basis space and an effective Hamiltonian[1] which gives an accounting of the positive-parity level structures of the entire sd-shell region. From this comparison of experiment with theory we attempt to learn both about the general characteristics of the conventional shell-model vis-a-vis electron scattering phenomena and about the specific model wave functions used to generate the theoretical form factors.

In the first instance, we look for systematic deviations between model predictions and experiment which can be remedied by alterations in the formulations of the electromagnetic operators. These alterations can be thought of as compensations for the restrictions of the model to a single oscillator shell and to purely nucleonic degrees of freedom. At their simplest, they would manifest themselves as shell-wide renormalizations of the strengths of the operators. Extensive knowledge on this aspect of the relationship between the conventional shell model and experimental data is available from comparisons of shell-model predictions and measured values of M1, E2 and Gamow-Teller matrix elements.

Electron scattering measurements make it possible to extend the range of such comparisons to higher multipoles. In practice, these are not observed in decay experiments. Of equal or greater importance, electron scattering also allows the momentum-transfer dependence of excitation processes to be examined. It is possible that the conventional shell-model approximations have consequences which are revealed as discrepancies between the predicted variations of multipole strength with momentum transfer q and the observed variations. Such discrepancies could be characterized as the need to employ q-dependent renormalizations to the operators.

In the second instance, we wish to test the specific assumptions about shell-model space and interaction which determine the actual wave functions used to generate the theoretical form factors. This we do by ascertaining whether the observed excitation strengths of the various multipoles which can participate in the scattering processes to the different final states are correctly predicted. The theoretical strengths are functions of the different mixings of the sd-shell configurations into the corresponding model states which occur in the diagonalizations of the Hamiltonian. These comparisons involved the relative strengths of the different allowed multipoles within a given transition, the relative strengths of a given multipole from transition to transition, and the overall normalizations of the transition strengths.

Obviously, the tests of the general characteristics of the shell-model approximation and of the specific individual wave functions are not completely disjoint. It is necessary to analyze an extensive set of related data with an internally consistent set of predictions before meaningful conclusions can be drawn independently about both of these aspects of nuclear structure theory. The ^{27}Al data of Ref. 2 and the wave functions of Ref. 1 provide necessary ingredients for such an analysis.

We show in Figs. 1 and 2, as examples of how theory and experiment compare, the form factors of the first and second $7/2^+$ stages of ^{27}Al, at excitation energies of 2.21 and 4.58 MeV respectively. The longitudinal (and total at 90^o) scattering to the lower state is observed to be dominated by the E2 multipole. The total scattering at $90^o$to the higher state (essentially all longitudinal, but a formal separation was not experimentally effected) is observed to be dominated by the E4 multipole. This observed qualitative change in dominance from E2 to E4 is in complete accord with the predictions for these two states. The experimental strengths with which the two states are excited (the maximum values of the form factors) are also accurately reproduced by the theoretical curves. Finally, the observed dependence of the excitation strengths upon the momentum transfer q are accurately reproduced over the range 0.5-2.5 fm^{-1}.

The theoretical form factors plotted in Figs. 1 and 2 incorporate single-particle wave functions of the harmonic-oscillator form, with the size parameter set to produce agreement with the measured rms charge radius, and simple "operator renormalizations" of the "effective charge" type. The values for these renormalizations are those obtained in surveys of B(E2) values and E2 and E4 electron scattering from double-even nuclei in the sd-shell. The E2 operator is effectively altered such that the model protons are assumed to have charges 1.35e and the model neutrons 0.35e. The E4 operator is

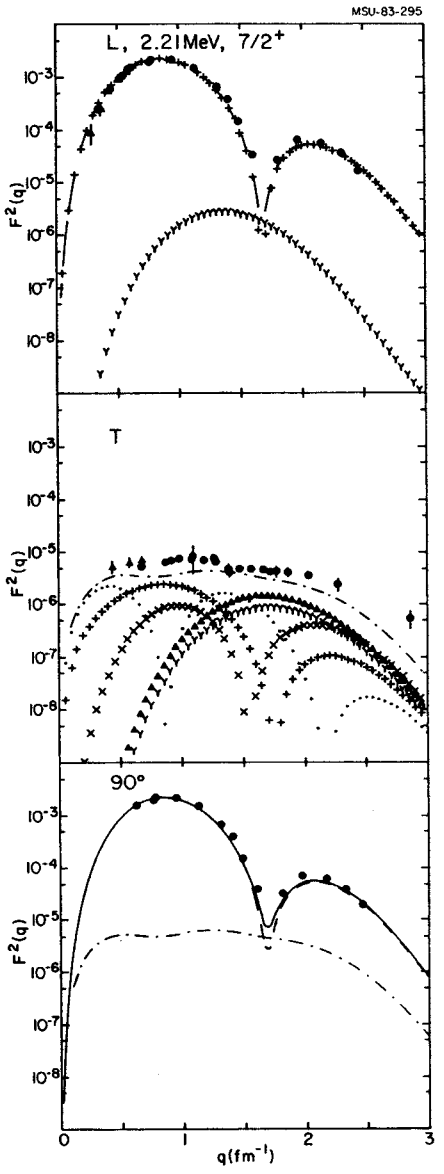

Fig. 1. Inelastic electron scattering form factors for the first $7/2^+$ state of ^{27}Al, which occurs at an experimental excitation energy of 2.21 MeV. The top panel shows the separated longitudinal form factor, the middle panel the separated transverse form factor and the bottom panel the total (unseparated) form factor at 90°. The lines show the full theoretical form factors in each case. The "+" and "Y" symbols in the longitudinal panel show the E2 and E4 components, respectively. In the transverse panel, the M1, E2, M3, E4 and M5 components are shown by the ".", "+", "x", "Y" and "triangle" symbols, respectively. In the 90° plot, the solid lines show the total, transverse plus longitudinal, form factor while the dashed-dotted line shows the transverse component alone, multiplied by the angular factor.

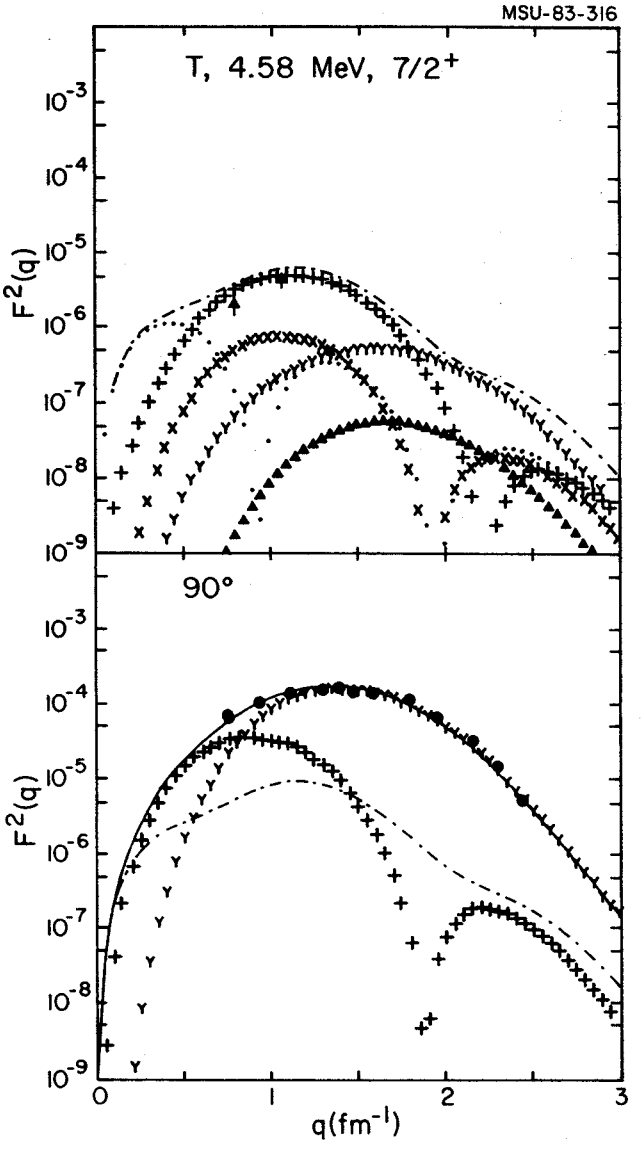

Fig. 2. Inelastic electron scattering from factors for the second $7/2^+$ state of ^{27}Al, which occurs at an experimental excitation energy of 4.58 MeV. The conventions of the presentation are the same as those used in Fig. 1.

altered such that the corresponding charges are 1.5e and 0.5e, respectively. The added charges are introduced in the form of transition densities which have the shape given by the Tassie model. In a sense, this can be taken as providing a q-dependent renormalization of the operator relative to the sd-shell configuration space transition densities.

We see from Figs. 1 and 2 that the wave functions correctly select out the dominant excitation multipoles, that the conventional effective charge values correctly normalize the strengths of these transitions and that the total model transition densities comprised of the valence sd-shell terms plus the Tassie-model core-polarization corrections successfully reproduce the form factors over the entire range of measured momentum transfer. We note also that the measured B(E2) of the electromagnetic decay between the first $7/2^+$ and the ground state is correctly reproduced with this same calculation.

The same two states are also populated by the transverse component of the electron

scattering process. The spins of the initial and final states are such that several multipoles can participate in the transitions. The envelopes of the theoretical sum of these multipole components agree reasonably well with the data for the two states. In addition, the measured B(M1) for the lower state is reproduced by the theory. The theoretical form factors incorporate the free-nucleon values of the charges and g-factors. The complexity of these particular data do not permit enough discrimination to determine if alterations to these normalizations are needed. Additional transverse measurements would allow more definitive conclusions on the apparent q-independence of the shell-model agreement with experiment.

---

1. B.H. Wildenthal, Bull. Am. Phys. Soc., 27, 725 (1982).
2. P.J. Ryan, R.S. Hicks, A. Hotta, J. Dubach, G.A. Peterson and D.V. Webb, Phys. Rev. C27, (1983).

SHELL MODEL CALCULATIONS OF SPECTROSCOPIC FACTORS AND ELECTROMAGNETIC PROPERTIES IN THE N=82 ISOTONES

H. Kruse and B.H. Wildenthal

We reported earlier on the computation of energy levels in the N=82 isotone chain of nuclei.[1] We have used the wave functions obtained in this work to determine spectroscopic factors and electromagnetic transition rates in the N=82 nuclei. We expect that these transition operators will provide a sensitive test of our wave functions. In addition the spectroscopic factors can provide some information on the nature of the subshell closure at ^{146}Gd.

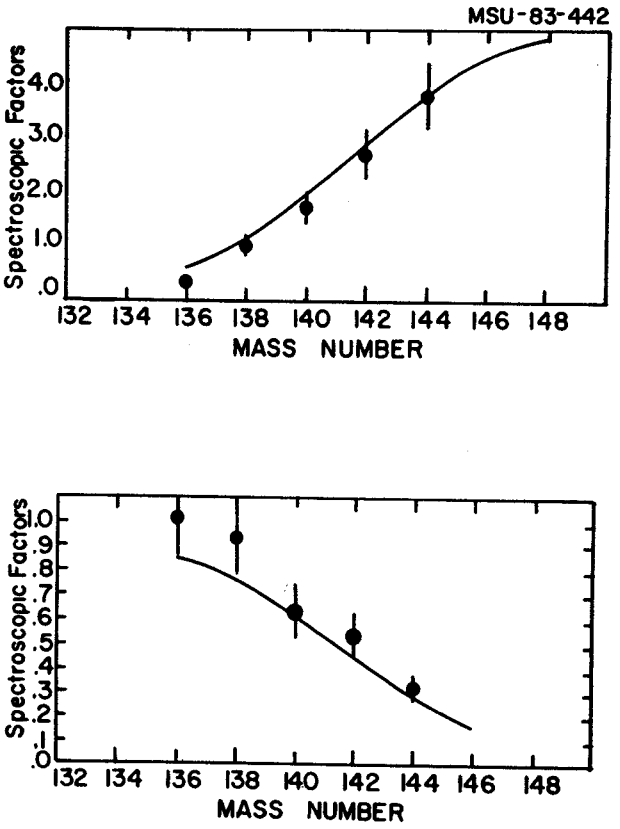

Fig. 1. (a) Experimental pickup strength from the $5/2^+$ orbit compared to the shell model prediction (solid line); (b) Same as (a), but for the stripping strength into the $5/2^+$ orbit.

Figure 1 shows one example for the computation of spectroscopic factors; shown is the stripping strength into the $5/2^+$ orbit as well as the pickup strength from the $5/2^+$ orbit. Note that the spectroscopic factor varies smoothly across the subshell closure, a trend which is also displayed in the data; this seems to indicate that the closure at Z=64 is a very soft one. This conclusion is supported by the pickup and stripping strengths for the remaining orbits.

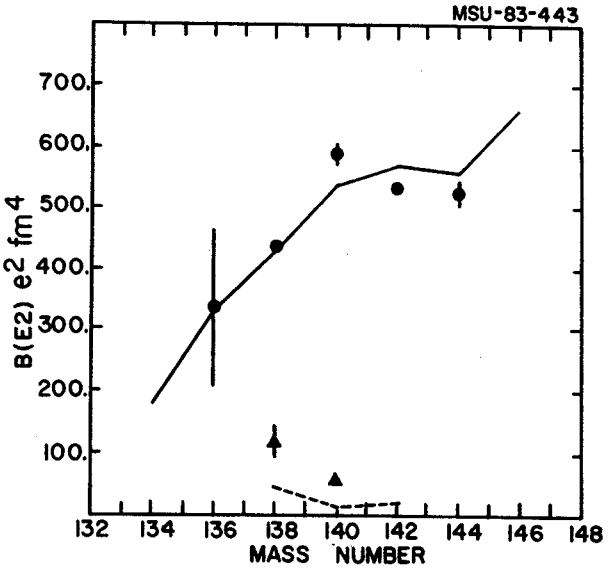

Fig. 2. Experimental B(E2) values for the $2^+)_1$ to $0^+)_1$ transition (circles) compared to the shell model result (solid lines); also shown is the comparison for the $4^+)_1$ to $2^+)_1$ transition (triangles and dashed line), both theoretical and experimental numbers were multiplied by 10 to be visible on this scale.

Figure 2 shows the B(E2) for the $4^+)_1$ to $2^+)_1$ and the $2^+)_1$ to $0^+)_1$ E2 transitions. The B(E2) values were computed using Wood-Saxon radial wave functions and an effective charge of e_{eff}=1.67. We note that the strong 2 to 0 transitions are in general well reproduced, whereas there are larger discrepancies in the weaker 4 to 2 transitions which sample small components of the nuclear wave functions.

A systematic study of electromagnetic transitions in the N=82 nuclei is currently in progress. We hope to use this information to improve our wave functions, add to the understanding of the electromagnetic properties of the nuclei in this region, and provide a guide for the interpretation of ongoing and future experiments involving electromagnetic transitions in these nuclei

1. H. Kruse and B.H. Wildenthal, Bull. APS 27, 533 (1982) and p. 725.

SPIN-TENSOR ANALYSIS OF NUCLEAR EFFECTIVE INTERACTIONS IN THE 1s-0d SHELL

B. A. Brown, W. A. Richter* and B. H. Wildenthal

* Permanent address: Physics Dept., University of Stellenbosch, Republic of South Africa.

The calculation of the shell-model effective interaction starting from the free nucleon-nucleon interaction remains one of the most important problems in nuclear physics. Considerable progress has been made in calculating the finite-nuclei reaction or G matrix. However, the renormalization of the bare G matrix required by the inevitable use of a truncated shell-model space is troubled by many uncertainties.[1] In this work we have compared the calculated effective two-body matrix elements based on the nucleon-nucleon interaction with the empirical matrix elements found from fits to binding energy data in the sd shell. The study is motivated in part by the need ror an effective interactions in heavier mass regions of a quality similar to those available for the 1s-0d shell. We hope that by thoroughly analyzing the features of the sd-shell interactions, the essential virtues of the empirical result can be translated to higher (larger) shell-model spaces.

The important physical aspects of the interaction can be more readily discerned by transforming the two-body j-j coupled matrix elements, which is the representation generally needed for shell-model calculations, to the L-S coupling scheme, following this by a spin-tensor decomposition. The essence of the spin-tensor decomposition method employed has been described by Kirson[2] and Yoro.[3] The two-body interaction can be written in the form

$$V = \sum_k V_k = \sum_k U^k \cdot S^k,$$

where the operators U and S are irreducible tensors of rank k in space and spin coordinates, respectively. In order to obtain the L-S coupled matrix elements, a j-j to L-S coupling transformation is applied:

$$\langle a\, b\, L\, S\, J\, T \mid V_k \mid c\, d\; L'\, S'\, J\, T \rangle$$

$$(2k+1) \begin{Bmatrix} L & S & J \\ S' & L' & k \end{Bmatrix} \sum_{J'} (-1)^{J'+k} (2J'+1) \begin{Bmatrix} L & S & J' \\ S' & L' & k \end{Bmatrix}$$

$$\{[(1+\delta_{ab})(1+\delta_{cd})]^{-1/2} \sum_{j_a', j_b', j_c', j_d'}$$

$$x[(2j_{a'}+1)(2j_{b'}+1)(2j_{c'}+1)(2j_{d'}+1)]^{1/2}$$

$$x \begin{Bmatrix} \ell_{a'} & 1/2 & j_{a'} \\ \ell_{b'} & 1/2 & j_{b'} \\ L & S & J' \end{Bmatrix} \begin{Bmatrix} \ell_{c'} & 1/2 & j_{c'} \\ \ell_{d'} & 1/2 & j_{d'} \\ L' & S' & J' \end{Bmatrix}$$

$$x[(1+\delta_{a'b'})(1+\delta_{c'd'})]^{1/2} \langle a'b'J'T|V_k|c'd'J'T\rangle\}$$

where $a = (n_a, l_a, j_a)$; $a' = (n_{a'}, l_{a'}, j_{a'})$, etc., in the matrix elements, and both two-body matrix elements are normalized and antisymmetrized. The nomenclature for the separated components is explained in the following table:

k	S	S'	Spin-tensor components
0	0	0	C = central
	1	1	
1	0	1	ALS = antisymmetric spin-orbit
	1	0	
	1	1	LS = spin-orbit
2	1	1	T = tensor

For the the 1s-0d shell the empirical effective matrix elements we have compared are those of Wildenthal (W),[4] Chung-Wildenthal-particle (CWP), Chung-Wildenthal-hole (CWH)[5,6] and Preedom-Wildenthal (PW).[7] The W matrix elements have a mass dependence of $(A/18)^{-0.3}$ and our comparisons are made for A=18. These are compared with the calculated bare (BK) and renormalized (RK) G-matrix elements of Kuo based in the Hamanda-Johnston potential,[8] as well as with the more recent results of Shurpin, Kuo and Strottman (SKS) based on the Reid soft-core (SKSR) and the Paris (SKSP) potentials.[9] The renormalized Kuo calculations include only the lowest second-order corrections, whereas the SKS calculations use the folded-diagram technique and includes 3rd and 4th order correction terms (we use the "C4" matrix elements of Ref. 9).

In the comparisons it should be remembered that the RK matrix elements were used as the starting parameters for the empirical matrix elements. For the PW and CW matrix elements only about 10 linear combinations of parameters were well determined from the experimental binding energies, whereas for the W interaction, 47 parameters were allowed to vary. Thus, we find in the comparison that the PW and CW matrix elements which were not well determined remain close to the BK values. The W matrix elements are much more independent of their origins. In order to get a completely independent set, as well as to obtain an estimate of the errors on the empirical matrix elements, we have repeated the fit based on 440

binding and excitation energy data which was used to obtain the W interaction, and allowed all 63 two-body matix elements and three single-particle matrix elements to vary (the BRW matrix elements). The values of the W and BRW matrix elements are essentially the same.

Our results are illustrated by the comparison of the central interaction components shown in Fig. 1. The 20 matrix elements are labeled by numbers (n) corresponding to the quantum numbers

n	ℓ_a	ℓ_b	ℓ_c	ℓ_d	L	S	T
1	2	2	2	2	1	0	0
2	2	2	2	2	3	0	0
3	2	0	2	0	2	0	0
4	2	2	2	2	0	1	0
5	2	2	2	2	2	1	0
6	2	2	2	2	4	1	0
7	2	2	2	0	2	1	0
8	2	2	0	0	0	1	0
9	2	0	2	0	2	1	0
10	0	0	0	0	0	1	0
11	2	2	2	2	0	0	1
12	2	2	2	2	2	0	1
13	2	2	2	2	4	0	1
14	2	2	2	0	2	0	1
15	2	2	0	0	0	0	1
16	2	0	2	0	2	0	1
17	0	0	0	0	0	0	1
18	2	2	2	2	1	1	1
19	2	2	2	2	3	1	1
20	2	0	2	0	2	1	1

The figure is divided into three panels. In each of the panels the BRW matrix elements are shown by circles with error bars connected by a solid line. In the top panel, BRW is compared with the PW (plus signs) and CWP (small dots connected by dashed lines) matrix elements. In the middle panel, BRW is compared to the SKS martix elements obtained from the Reid soft-core potential (plus signs) (SKSR) and the Paris potential (SKSP) (small dots connected by dashed lines). In the bottom panel, BRW is compared to the RK (plus signs) and BK (small dots connected by dashed lines) matrix elements of Kuo.

In this comparison we can note the following: All empirical matrix elements are well determined except for those with (S,T)=(0,0) which have relatively large error bars. The differences between the empirical BRW, PW and CWP matrix elements are surprisingly small given the superiority of BRW (W) over PW and CW in reproducing sd shell binding energies and excitation energies. The differences between the G-matrix elements obtained from the Reid (SKSR) and Paris (SKSP) potentials are small compared to the differences between the original Kuo (RK) and the new (SKSR) results. This illustrates that the major uncertainty lies in the renormalization calculations and probably not in the nucleon-nucleon interaction. In the Kuo calculation the renormalizaton is important to obtain improved agreement with BRW. The renormalization is not as large in the more complete SKS calculation, and

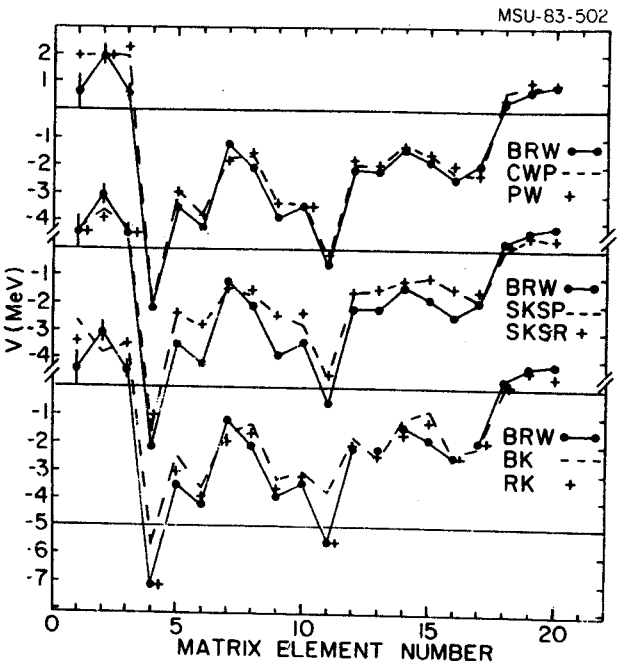

unfortunately the agreement with BRW becomes worse. The repulsive (S,T)=(0,0) and (1,1) SKS matrix elements are in reasonable agreement with BRW, but the important attractive (S,T)=(0,1) and (1,0) SKS matrix elements are too weak compared to BRW.

Similar comparisons have been made with the other components of the interaction. From these comparisons we hope to obtain an improved method of calculating reliable effective interactions to be used in nuclear-structure calculations.

References

1. T.T.S. Kuo, Ann. Reviews of Nucl. Sc. 24, 101 (1974).
2. M.W. Kirson, Phys. Lett. 47B, 110 (1973).
3. K. Yoro, Nucl. Phys. A333, 67 (1980).
4. B.H. Wildenthal, Bull. Am. Phys. Soc. 27, 725 (1982).
5. W. Chung, Ph.D. Thesis, Michigan State University (1976).
6. B.H. Wildenthal, Elementary Modes of Excitation in Nuclei, edited by R. Broglia and A. Bohr (Soc. Italiana de Fisica, 1977).
7. B.M. Preedom and B.H. Wildenthal, Phys. Rev. C6, 1633 (1972).
8. T.T.S. Kuo, Nucl. Phys. A103, (1967).
9. J. Shurpin, T.T.S. Kuo and D. Strottman, preprint 1983.

SHELL-MODEL STUDY OF THE (p,π^-) REACTIONS IN THE $f_{7/2}$-SHELL REGION

B. A. Brown, O. Scholten and H. Toki

MSU-83-325

Recently the results of a series of (p,π^-) experiments on a number of nuclei have been reported by the Indiana group (Vigdor et al.)[1] They have pointed out that this reaction populates selective high spin states which can be correlated in many instances with those identified previously in gamma decay and particle transfer experiments. In addition, they have found evidence from analyzing power measurements that this reaction involves a relatively simple two-nucleon pion production process.[2] For the Ca isotopes and the N=28 isotones, the (p,π^-) cross sections for populating discrete low-lying final states have a strong dependence on N and Z. The cross sections integrated over the strong states below 5 MeV excitation energy in the final nucleus for 206 MeV protons and a pion emission angle of 30° are in units of nb/sr 10.6±1.3 for ^{43}Ti, 8.8±2.0 for ^{45}Ti, 53.2±1.4 for ^{49}Ti, 18.0±3.0 for ^{51}Cr and 9.9±1.5 for ^{53}Fe.[3]

The final states most strongly populated in the ^{48}Ca$(p,\pi^-)^{49}$Ti reaction comprise a doublet,[4] the higher member of which is consistent in energy with the $19/2^-$ state at 4.4 MeV excitation energy observed in a gamma decay experiment.[5] However, the lower peak, at 4.0 MeV, cannot be associated with any high-spin state previously identified. Moreover, in a recent experiment with 165 MeV protons,[4] the pions from these two states have been observed to have quite different angular distributions. The cross section of the 4.4 MeV peak falls off by about a factor of two over the angular range of 30-135° while the cross section of the 3.9 MeV peak falls by off about an order of magnitude in the same angular range.

We have found that all of the above features of the relative cross sections for these nuclei can be qualitatively understood within the contexts of the $(1f_{7/2})^n$ shell model and some general assumptions about the reaction mechanism in the plane-wave Born approximation limit. From the basic Feynman diagrams for this reaction shown in Fig. 1 it is clear that the reaction involves three nucleons. The box at the outgoing pion line in Fig. 1 can be the s-wave and/or p-wave vertex.[6] As the proton energy increases, the p- wave process with a delta-isobar intermediate state excitation becomes dominant.[6,7] The general nuclear structure amplitude for this reaction can

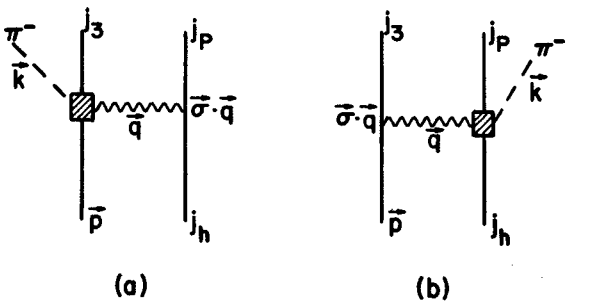

Fig. 1. Feynman diagrams for the (p,π^-) reaction. The incoming proton is repesented by a solid line with momentum p and is transfered into a bound orbit in the nucleus j_3. j_p and j_h are the orbits of the particle-hole states. The dotted line denotes the outgoing pion with momentum k and the intermediate boson with momentum q is denoted by a wavy line.

be expressed in terms of matrix elements of creation and annihilation operators. In order to separate the spatial and spin degrees of freedom it is useful to express these amplitudes in LS coupling

$$A(i,f,L_{ph},S_{ph},L,S,J,n_p,n_h,n_3,\ell_p,\ell_h,\ell_3,r) =$$

$$\sum_{J_{ph},j_p,j_h,j_3} \begin{Bmatrix} \ell_p & \ell_h & L_{ph} \\ 1/2 & 1/2 & S_{ph} \\ j_p & j_h & J_{ph} \end{Bmatrix} \begin{Bmatrix} L_{ph} & \ell_3 & L \\ S_{ph} & 1/2 & S \\ J_{ph} & j_3 & J \end{Bmatrix}$$

$$\times \langle f||[[a^+(\pi\alpha_p)\times\tilde{a}(\nu\alpha_h)]^{J_{ph}} \times a^+(\pi\alpha_3)]^J||i\rangle F(r)$$

where $F(r) = R(\alpha_p,r)\, R(\alpha_h,r)\, R(\alpha_3,r)$ (i/f)

stands for the quantum numbers of the initial and final states and α stands for the set of quantum numbers (n,ℓ,j) of the shell-model orbits. [] is the normalized 9-j coefficient. In the cases of interest here $\alpha_p = \alpha_h = \alpha_3 = 1f_{7/2}$, $J_i = 0$ and hence $J = J_f$ for the total angular momentum transfer. In our $(j)^n$ case and in the zero-range approximation used below the total spin transfer can only be S=1/2 which can be understood by first coupling the two protons to spin S_{pp}. Since the two protons are in the same orbit, $S_{pp}=0$ and thus S=1/2. In order to conserve parity in the zero-range approximation, L must be odd, and thus each final state spin has a unique total L transfer given by $L = J \pm 1/2$. These amplitudes have been calculated with the wave functions obtained with the "^{42}Sc" interaction of Ref. 8. A harmonic oscillator potential with $\hbar\omega = 10.5$ MeV was used for the bound-state radial wave function R(r).

Since the major part of this momentum has to be carried away by the interaction line in Fig. 1, the interaction is of short range and the zero-

range approximation should be adequate. A plane wave calculation for the incoming proton and outgoing pion then leads to the following expression for the cross section

$$\frac{d\sigma}{d\Omega} = \sigma_0(2J_f+1) \sum_{L,S,J} \{ \sum_{L_{ph},S_{ph},n_i,\ell_i} \varepsilon(S_{ph})$$

$$[(2\ell_p+1)(2\ell_h+1)(2\ell_3+1)/(2L+1)]^{1/2}$$

$$\times(\ell_p 0 \ell_h 0|L_{ph}0)(L_{ph}0\ell_3 0|L0)$$

$$\times \int A(i,f,L_{ph},S_{ph},L,S,J,n_i,\ell_i,r) j_L(qr) r^2 dr \}^2$$

For our one-orbit calculation it can be shown that $A(S_{ph}=1) = (3)^{1/2} A(S_{ph}=0)$ and hence the ε dependence enters in our case just as an overall scale factor (independent of angle) in the cross sections. (The results presented here were obtained with $\varepsilon(S_{ph}=1)=1$ and $\varepsilon(S_{ph}=0)=0$).

The reaction will be peaked at the nuclear surface because of the strong pion absoption. This can be taken into account in an approximate fashion by using a lower cutoff in the above radial integral. The angular distributions are in fact rather sensitive to this cut-off. We have chosen the value of 3.3 fm (about 1.1 $A^{1/3}$), which gives the best reproduction of the experimental $^{48}Ca(p,\pi^-)$ angular distributions. The momentum transfer as a function of angle is $q = |p_{eff} - k_{eff}|$ where the effective momenta take into account the Coulomb energy at the nuclear surface. The most important aspect of the kinematics is the large momentum mismatch. For E_p = 200 MeV, the angular momentum transfer for the pions outgoing at 0° is $\Delta\ell = R_0 \Delta p = 11$ for ^{48}Ca (and is as large as 17 for backward angles). Hence, this reaction excites high spin states (high orbital angular momentum states) almost exclusively.

The cross sections (ignoring the relatively small Q-value dependence in the radial integral) for a given L transfer (L≠3) are proportional to the probability of stripping two protons into an $f_{7/2}$ orbit with $L_{pp}\neq 0$ multiplied by the probability of picking up a neutron from an $f_{7/2}$ orbit. For the $(f_{7/2})^n$ seniority-zero ground configurations of the Ca isotopes and N=28 isotones it can be shown that this spectroscopic sum rule is proportional to (N-20)(28-Z)(26-Z) for each L(≠3) for N and Z of the target. For the cases of interest these numbers are proportional to 12 for ^{43}Ti, 24 for ^{45}Ti, 48 for ^{49}Ti 24, for ^{51}Cr and 8 for ^{53}Fe. Except for ^{45}Ti, these values are closely proportional to the experimental cross sections noted above.

The calculated spectra for E_p = 206 MeV and pions at 30° are shown in Fig. 2. The agreement with experiment[1,3,4] is excellent. Several details of the spectra which have not been previously understood come out of our calculations. In the theoretical ^{49}Ti spectrum there are only two strong states one $15/2^-$(L=7) and one $19/2^-$(L=9). They agree in energy with the two states observed experimentally within a few hundred keV. Since they have different L transfer values, the angular distributions are very different and at 100° the $19/2^-$(L=9) state dominates the spectra. The $19/2^-$(L=9) state is much stronger than the $17/2^-$(L=9) state because

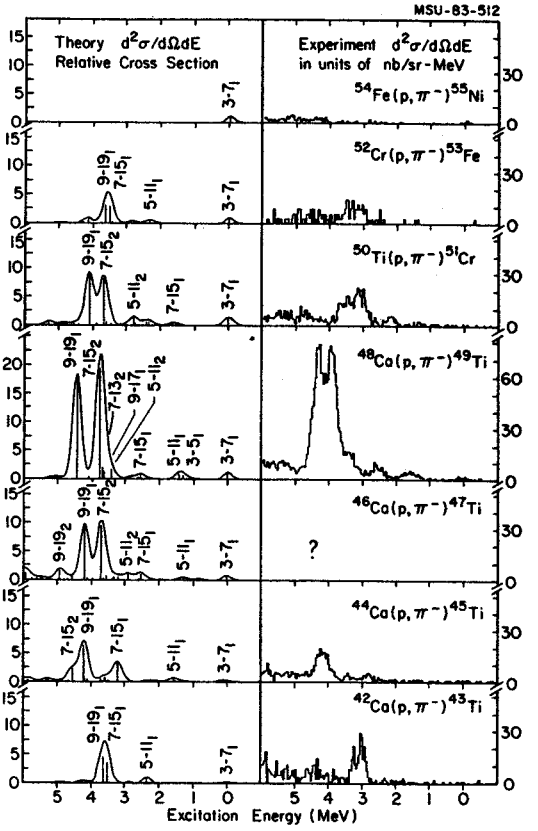

Fig. 2. Comparison of the experimental (p,π^-) cross sections for E_p=206 MeV and pions at 30° (Ref. 4) with the calculated relative cross sections (σ_0=1000). The location of the strong peaks in the theoretical spectra are labeled by $L\text{-}2J_n$ where n indicates the nth state of spin J. The theoretical smooth line represents a Gaussian average with Γ_{FWHM}=0.3 MeV which takes into account the finite resolution in the experiment. Above 6 MeV in excitation energy there are no strong states in the theoretical spectra and the experimental spectra show a smoothly rising background (Ref. 1).

the latter is unfavored in the jj to LS transformation (this same difference between $19/2^-$ and $17/2^-$ also occurs, for the same reason, in three nucleon transfer.[9]) Whereas the lowest $15/2^-$(L=7) state is strong in ^{43}Ti, it is the second $15/2^-$ state which is strong in ^{49}Ti. This is due to the change in going from particle-particle to the particle-hole structure in the wave functions. This feature of the $15/2^-$ states in ^{49}Ti is confirmed by comparisons with gamma decay data,[5] in which only the yrast $15/2^-$ state is seen, and by comparison with recent ^{51}V(d,α) data,[10] in which both $15/2^-$ states (and other high-spin states) are seen with relative strengths in agreement with $(f_{7/2})^n$ calculations. Finally we note the fraction of the total L=7 and L=9 strength concentrated in the low-lying strong states for the five final nuclei (A) of interest are 92%(43), 62%(45), 89%(49), 83%(51) and 91%(53). This increased fragmentation in ^{45}Ti explains most of the deviation in this case from the trends expected from the sum rules noted above (the remaining strength in ^{45}Ti is fragmented over many levels but mainly into the T=3/2, $J^\pi = 15/2^-$ and $19/2^-$ states around 10 MeV in excitation).

The features of the spectra are dominated by an "ℓ-window" created on the lower side by the momentum mismatch in the reaction and on the higher side by the maximum transfer (L_{max}=9) available for three particles in the fp shell. It will thus be interesting to pursue experimentally the (p,π^-) reaction on ^{88}Sr (L_{max}=12) and on ^{144}Sm (L_{max}=15). In ^{89}Zr we expect a cluster of three closely spaced states with L=12, 10 and 8 around 4 MeV in excitation. (More angular momentum transfer can be achieved by putting the proton into the higher shells and this process may be part of the continuum seen above the discrete states). The success of our simple calculations should encourage progress in the developement of distorted wave calculations. Indeed, because of the selectivity of this reaction, a great deal may be learned from such calculations about the the interactions of pions in nuclei.

References

1. S. E. Vigdor et al., Phys. Rev. Lett. 49, 1314 (1982).
2. W. W. Jacobs et al., Phys. Rev. Lett. 49, 855 (1982).
3. S. E. Vigdor et al., contributed paper to the International Conference on Nuclear Structure, edited by A. van der Woude and B. J. Verhaar, Amsterdam September 1982, Nucl. Phys. A396, 61c (1983).
4. T. G. Throwe et al., Bull. Am. Phys. Soc. 28, 672 (1983) and private communication.
5. M. Behar et al., Nucl. Phys. A366, 61 (1981).
6. W. Kutchera, B. A. Brown and K. Ogawa, Revista del Nuovo Cimento, Serie 3, Vol 1, N. 12 (1978).
7. E. Oset, H. Toki and W. Weise, Phys. Rep. 83, 281 (1982).
8. J. Chai and D. O. Riska, Nucl. Phys. A329, 429 (1979).
9. R. Kouzes, et al.,, Bull. Am. Phys. Soc. 28, 705 (1983), and private communication from H. Nann and R. Sherr.
10. P. A. Smith et al., Phys. Rev. C18, 2065 (1978).

A CALCULATION OF THE CONTINUUM IN (p,π^-) SCATTERING

O. Scholten and H. Toki

Recently the interest in the (p,π^-) reaction has been growing.[1] It has been demonstrated to be a valuable tool in spectroscopic studies.[2] In order to make full use of it as a spectroscopic tool, the origin of the continuum has to be understood. At 200 MeV the (p,π^-) spectrum has been measured up to an excitation energy of about 20 MeV for different targets.[1] The continuum turns out to have a rather peculiar structure, it rises linearly with excitation energy starting at about E_x=5 MeV.

We have calculated the continuum in a simple fermi-gas model assuming that the process goes via a Δ intermediate state. For forward angle scattering the cross section can be written as

$$\frac{d\sigma}{d^3q_\pi} = \frac{1}{(2\pi)^3}\int \frac{d^3k_n}{(2\pi)^3}\frac{d^3k_p}{(2\pi)^3}(2\pi)^4\delta^4(k_n+k_p+q_\pi)$$

$$\frac{d^4q_\pi}{(2\pi)^4}\frac{d^3k_{p_2}}{(2\pi)^3}(2\pi)^4\delta^4(P_{tot})\frac{1}{2\omega_\pi}f^2_{NN\pi}f^4_{N\Delta\pi}\frac{1}{m_\pi^6}$$

$$\frac{q_\pi^2}{(\omega-\omega_0)^2+\Gamma^2/4}(8/9)^2$$

We have made here the approximation that the momentum transfer q is large, such that the interaction can be approximated by a δ function. The integration limits are determined by the fact that k_n should lie inside the fermi sea while k_p and k_{p_2} have to be above. The integral over the particle hole states, k_n and k_p, give rise to the particle hole response of a fermi gas which can be written as the imaginary part of the Lindhard function. After this substitution only a two dimensional integral remains to be done numerically. In Fig. 1 the caluclated continuum is shown. By comparing with the date given in Ref. 1 it can be seen that a qualitative agreement is obtained. The next stage of the calculations is to reproduce the absolute cross section. Preliminary calculations look promising.

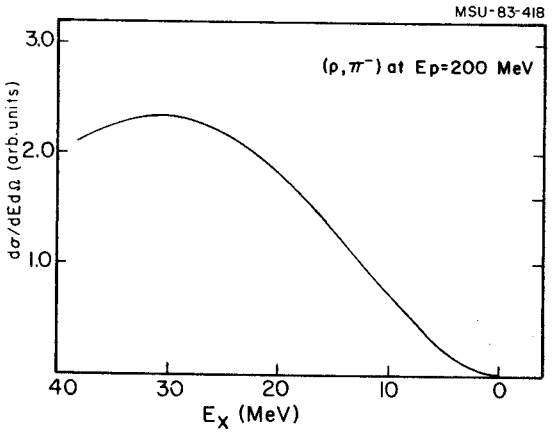

Fig. 1. Calculated continuum cross section for (p,π^-) at 200 MeV in a fermi gas model.

1. IUCF newsletter 31, October 1982.
2. B.A. Brown, O. Scholten and H. Toki, to be published.